

LCF Properties Investigation of Sn-3.5Ag-0.75Cu Solder Paste

ANTOŠ D.^{1,a}, HALAMA R.^{1,b}, MARKOPOULOS A.^{1,c}

¹Department of Applied Mechanics, Faculty of Mechanical Engineering, VŠB – Technical University of Ostrava, 17. listopadu 2172/15, 708 00 Ostrava, Czech Republic

^adaniel.antos.st@vsb.cz, ^bradim.halama@vsb.cz, ^calexandros.markopoulos@vsb.cz

Keywords: Sn-3.5Ag-0.75Cu, solder paste, low-cycle fatigue, viscoplasticity

Abstract.

This study is focused on research in tension-compression fatigue and uniaxial ratcheting. Strain controlled fatigue tests were done under constant strain amplitude loading considering a constant strain rate on a specially designed specimen. The influence of the mean stress and the stress amplitude on uniaxial ratcheting has been studied for three load frequencies. Results are consistent with the stress-strain behaviour observed under monotonic loading. Aim of this and previous investigations is to obtain experimental data of Sn-3.5Ag-0.75Cu solder paste for calibration of a viscoplastic material model for future finite element analysis and to propose appropriate fatigue damage model for subsequent computational fatigue analysis. First results gained by a non-unified constitutive model are also presented.

Introduction

Tin based materials show strongly rate dependent stress-strain behaviour. Most of the studies which investigate the lead-free solder paste mechanical properties are mainly focused on rate-dependent and thermal-dependent plasticity in monotonic loading [1] or secondary creep properties [2]. Uniaxial low-cycle fatigue was investigated for example by Ohguchi et al [3], but only stabilized hysteresis loops were published. The transient behavior seems to be out of scope for most of scientific studies. There are only few published works emphasized on accumulation of plastic strains due to non-zero mean stress (ratcheting), for example [4], [5].

This study follows the contributions, which were focused on measurement of mechanical properties in monotonic tension, monotonic torsion and creep [6] and low cycle fatigue in torsion of a lead-free solder paste [7].

Experiment description

First, LCF tension-compression fatigue tests were performed for the constant strain rate of $0.015 \text{ mm}\cdot\text{s}^{-1}$. Special solderjoint specimens were manufactured [6]. Dog bone round cross-section specimens consist of two copper pieces between which 0.5mm of solder paste Sn-3.5Ag-0.75Cu was applied [6]. The number of cycles to failure was evaluated according to the criterion of the percentage drop in tensile force in relation to the level determined during the measurement. The percentage drop value is typically in range from 2% to 30% [8]. In our case, the crack initiation was determined as the number of cycles corresponding to a 20% force reaction drop of extrapolated force over the upper curve of tensile force vs. number of cycles. In the Fig. 1, the main results of the test evaluation are shown, whereas the number of cycles to failure was determined to 85. There is also presented the uniaxial hysteresis loop in half-life on the right side of the Fig.1.

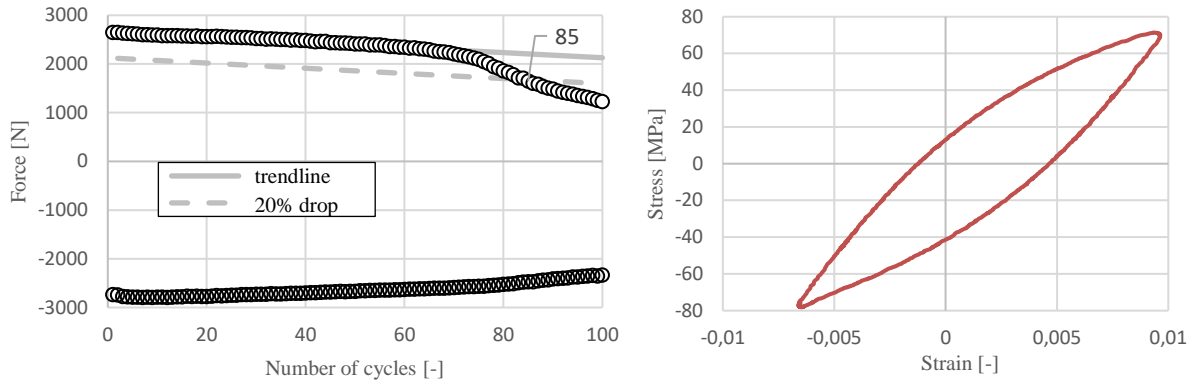


Fig. 1: Evaluation of the crack initialization (left), half-life hysteresis loop (right)

These tension-compression fatigue tests were performed for four strain amplitude levels. Strain amplitudes from hysteresis loops in the half-life were used to construct the e-N curve (Fig. 2). The stiffness of copper parts was taking into account in evaluations considering Hooke's law with elastic properties of copper (Young modulus $E=137.6$ GPa, Poisson ratio $\nu=0.34$).

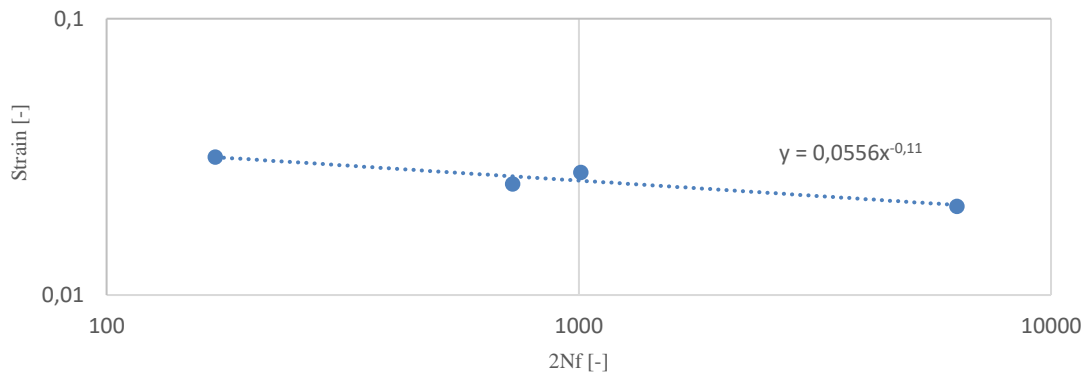


Fig. 2: Lifetime curve for Sn-3.5Ag-0.75Cu of tension-compression fatigue

The second study will presents the influence of mean stress and stress amplitude on the accumulation of axial strain in specimens. Uniaxial ratcheting was investigated for three different loading frequencies 0.25Hz, 0.35Hz and 0.5Hz. The test consisted of seven loading blocks. In the first three loading blocks with duration of 50 cycles per block, the force amplitude was incrementally increased while mean force value remained the same. In the following four loading blocks with duration of 25 cycles per block, the mean force value was step-wisely increased while force amplitude remained constant, see Table 1.

Table 1: Uniaxial ratcheting test conditions

Number of cycles per set	50	50	50	25	25	25	25
Force amplitude (N)	1500	1650	1800	1800	1800	1800	1800
Mean force (N)	200	200	200	250	300	350	400

The influence of stress amplitude on ratcheting in solderjoint was obtained from first three blocks in each test (Fig.3 left). The ratcheting strain is evaluated from measured elongation on 25 mm gauge length after subtracting elastic deformation of copper parts and considering the solderjoint thickness. From following blocks, the dependency of the mean stress on the ratcheting strain rate in solderjoint has been evaluated (Fig.3 right). The impact of mean stress as well as stress amplitude on ratcheting rate is almost linear in particular lower stress intervals.

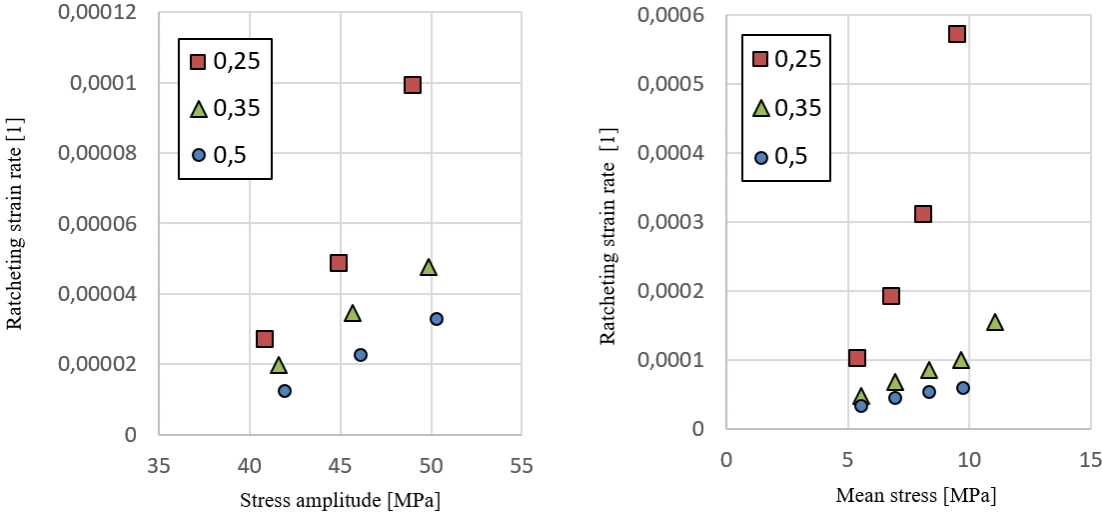


Fig. 3: Dependency of the ratcheting strain rate on stress amplitude (left) and dependency of the ratcheting strain rate on mean stress (right)

Viscoplastic model calibration

Data from described fatigue tests will be used to validate a viscoplastic material model using FE analysis. In this paper, we focused on the calibration of the non-unified material model [9] implemented into the ANSYS 2020R1 by a user-subroutine written in Fortran. AbdelKarim-Ohno kinematic hardening rule was also introduced in order to describe ratcheting behaviour properly. Basic constitutive model equations and material parameters optimized by analytical formulas based on experimental data from literature [3] are stated in Table 2 and Table 3 respectively. The results of predictions are shown in the Fig. 4. The advanced material model for capturing transient cyclic behaviour will be used also in a future study for simulations of fatigue tests presented here.

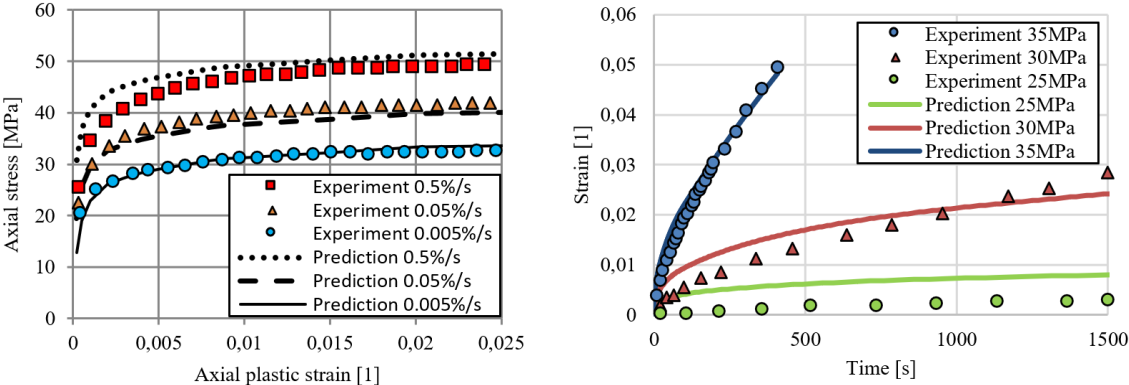


Fig. 4: Calibrated advanced material model considering monotonic tensile curves (left) and creep curves for Sn-3.5Ag-0.75Cu (experiment taken from [3])

Table 2: Viscoplastic non-unified model description

$$\begin{aligned}
 \boldsymbol{\varepsilon} &= \boldsymbol{\varepsilon}^e + \boldsymbol{\varepsilon}^{tr} + \boldsymbol{\varepsilon}^{ss}, \\
 \boldsymbol{\sigma} &= \mathbf{D}^e : \boldsymbol{\varepsilon}^e, \\
 \dot{\boldsymbol{\varepsilon}}^{tr} &= \frac{2}{3} \cdot g^{tr}(\bar{y}, p) \cdot \frac{\mathbf{s} - \mathbf{a}}{\bar{y}}, \quad g^{tr} = A^{tr} \bar{y}^{m^{tr}}, \\
 \dot{\boldsymbol{\varepsilon}}^{ss} &= \frac{2}{3} \cdot g^{ss}(\bar{s}) \cdot \frac{\mathbf{s}}{\bar{s}}, \quad g^{ss} = A^{ss} \bar{s}^{m^{ss}}, \\
 \mathbf{a} &= \sum_{i=1}^M \mathbf{a}^i, \\
 \dot{\mathbf{a}}^i &= \frac{2}{3} h^i \cdot \dot{\boldsymbol{\varepsilon}}^{tr} - \mu \cdot \xi^i \cdot \mathbf{a}^i \cdot \dot{p} - H(f^i) \cdot \xi^i \cdot \langle \dot{\lambda}^i \rangle \cdot \mathbf{a}^i, \\
 \dot{\lambda}^i &= \dot{\boldsymbol{\varepsilon}}^{tr} : \frac{\mathbf{a}^i}{h^i \xi^i} - \mu \dot{p}, \quad f^i = \frac{3}{2} \mathbf{a}^i : \mathbf{a}^i - \left(\frac{h^i}{\xi^i} \right)^2, \\
 \bar{y} &= \sqrt{\frac{3}{2}} \|\mathbf{s} - \mathbf{a}\|, \quad \bar{s} = \sqrt{\frac{3}{2}} \|\mathbf{s}\|, \quad \dot{p} = \sqrt{\frac{2}{3}} \|\dot{\boldsymbol{\varepsilon}}^{tr}\|,
 \end{aligned}$$

where $\langle x \rangle$ means the Macaulay bracket ($\langle x \rangle = (x + |x|)/2$), $H(f^i)$ is the Heaviside step function and $\boldsymbol{\varepsilon}^e, \boldsymbol{\varepsilon}^{tr}, \boldsymbol{\varepsilon}^{ss}$ - elastic, transient and steady state strain tensors

$\boldsymbol{\sigma}, \mathbf{s}$ - stress tensor and its deviatoric part

\mathbf{a}, \mathbf{a}^i - backstress and its i -th part

\mathbf{D}^e - material elastic stiffness 4th order tensor

\bar{y}, \bar{s} - effective and equivalent stress

p - accumulated plastic strain

M - number of backstress parts

Table 3: Material parameters obtained for Sn-3.5Ag-0.75Cu

$$\begin{aligned}
 E &= 29500 \text{MPa}, \quad \nu = 0.35, \quad A^{tr} = 7.2e - 9, \quad m^{tr} = 4.1, \quad A^{ss} = 5e - 25, \quad m^{ss} = 12, \quad \mu = 0.1 \\
 h^1 &= 14000 \text{MPa}, \quad \xi^1 = 2000, \quad h^2 = 4000 \text{MPa}, \quad \xi^2 = 1000, \quad h^3 = 1800 \text{MPa}, \quad \xi^3 = 600, \\
 h^4 &= 675 \text{MPa}, \quad \xi^4 = 450, \quad h^5 = 500 \text{MPa}, \quad \xi^5 = 250, \quad h^6 = 375 \text{MPa}, \quad \xi^6 = 125, \\
 h^7 &= 200 \text{MPa}, \quad \xi^7 = 50, \quad h^8 = 20 \text{MPa}, \quad \xi^8 = 20
 \end{aligned}$$

Conclusions

The experimental program of Sn-3.5Ag-0.75Cu solder paste has been briefly described. The low-cycle fatigue tests realized under strain control will serve as a basis for identification of appropriate fatigue criterion. The response of considered lead-free solder paste reveals ratcheting with steady state. The ratcheting tests show important relationship between ratcheting rate and mean stress as well as stress amplitude.

With regard to stress-strain behaviour observed in the experimental campaign the most powerful nonlinear kinematic hardening rule has been stated according to AbdelKarim-Ohno [10]. Separate flow rules have been introduced leading to a non-unified theory. Material parameters of the advanced viscoplastic model were identified using data from literature based on analytical relations. The calibrated material model will be used in future simulation of fatigue tests.

Based on stress-strain history from described fatigue tests the viscoplastic material model will be calibrated for elevated temperatures. The optimization task will be done using the optiSlang software [11] similarly as presented elsewhere for Anand's viscoplastic model [12].

Acknowledgement

This work was supported by The Ministry of Education, Youth and Sports from the Specific Research Project (SP2020/23) by The Technology Agency of the Czech Republic in the frame of the project TN01000024 National Competence Center-Cybernetics and Artificial Intelligence and the Grant Agency of the Czech Republic (GACR) project No. 19-03282S. The support of Continental Automotive Czech Republic company is also acknowledged.

References

- [1] M. Motalab, Z. Cai, J. C. Suhling, P. Lall, Determination of Anand constants for SAC solders using stress-strain or creep data, Proceedings of the 13th IEEE ITherm Conference, San Diego, CA, May 30 - June 1, 2012, pp. 910-922.
- [2] M. Amagai, Characterization of chip scale packaging materials, Microelectronics Reliability 39 (1999) 1365-1377.
- [3] K. Ohguchi, K. Sasaki, M. Ishibashi, T. Hoshino, Plasticity-creep separation method for viscoplastic deformation of lead-free solders, JSME Int. J. Series A 47/3 (2004) 371-379.
- [4] K. Sasaki, K. Ohguchi, Uniaxial ratchetting behavior of solder alloys and its simulation by an elasto-plastic-creep constitutive model. Journal of Elec. Materi. 40 (2011) 2403.
- [5] T. Kobayashi, K. Sasaki, Experiments and simulations of uniaxial ratchetting deformation of Sn-3Ag-0.5Cu and Sn-37Pb solder alloys, J. Mater. Sci.: Mater. Electron. 20 (2009) 343-353.
- [6] D. Antoř, R. Halama, M. Bartecký, Measurement of mechanical properties of lead free alloy, In: Proceedings of 56th International conference on Experimental Stress Analysis 2018 (EAN2018), Hotel Sklář, Harrachov, 2018, Czech Republic.
- [7] D. Antoř, R. Halama, M. Bartecký, Cyclic Plastic Properties of a Lead Free Solder, Key Eng. Mater. 810 (2019) 46-51.
- [8] ČSN ISO 12106, Kovové materiály - Zkoušení únavy - Metoda řízení osově deformace.
- [9] M. Kobayashi, M. Mukai, H. Takahashi, N. Ohno, T. Kawakami and T. Ishikawa, Implicit integration and consistent tangent modulus of time-dependent non-unified constitutive model, Int. J. Numer. Meth. Eng. 58 (2003) 1523-1543.
- [10] M. Abdel-Karim, N. Ohno, Kinematic hardening model suitable for ratchetting with steady-state. Int. J. Plast. 16 (2000) 225–240.
- [11] ANSYS optiSLang, Dynardo, 2020, <https://www.dynardo.de/en/software/optislang.html>
- [12] D. Antoř, R. Halama, Viscoplastic modeling of stress-strain behavior of a lead free solder, Proceedings of Applied Mechanics 2019 conference, Ostravice, April 15-17, 2019, Czech Republic.